

Supplemental Methods

Antibodies

A list of all mass cytometry antibodies and reporter isotopes is included in Supplemental Table 2. A subset of the antibodies was purchased pre-conjugated from Fluidigm (formerly DVS Sciences). Candidate reagents for the CyTOF panel were first tested in flow cytometric assays on defined tumor cell lines and normal donor peripheral blood mononuclear cells (PBMCs) and/or *in vitro* activated T cells and polarized macrophages. A high performing antibody provided a specific signal in the positive control, which was absent in the negative control with minimal background.

Antibodies were conjugated to specific isotopes using the web-based Fluidigm panel designer to select channels with optimal signal and minimal background from oxidation and neighboring channel leakage¹. For primary conjugations, purified antibodies were obtained in carrier protein-free PBS and labeled using the X8 polymer MaxPAR antibody conjugation kit (Fluidigm) according to the manufacturer's protocol. Two purified metal isotopes, Indium 113 and 115 (Trace Sciences), were purchased separately and conjugated using buffers from Fluidigm X8 polymer kit.

All metal-labeled antibodies were diluted, based on their percent yield by measurement of absorbance at 280nm, to between 0.2 and 0.4 mg/mL in Candor PBS Antibody Stabilization solution (Candor Biosciences, GmbH) and stored at 4°C. Each antibody clone and lot was titrated to optimal staining concentrations using a panel of cHL cell lines (L428, KMH2, HDLM-2, L540 and L1236 (DSMZ, German cell line collection)), normal PBMCs and *in vitro* activated T cells or polarized macrophages.

PBMC Isolation

Peripheral blood mononuclear cells were obtained from leukapheresis collars via a Ficoll-Paque PLUS (GE Healthcare) gradient. Cells were diluted 3 fold with PBS and layered over 15 mL of Ficoll-Paque and centrifuged at 400g for 30 mins at 20°C in a swinging-bucket rotor without brakes. PBMCs were carefully transferred to a fresh tube and washed with PBS by centrifugation. The pellet was resuspended in complete RPMI-1640 media to create a single cell suspension.

***In vitro* activation of normal T cells**

T-cells were purified from PBMCs by a 2-step magnetic bead negative selection according to manufacturer's protocol (Miltenyi Biotec). T-cells were resuspended in RPMI-1640 supplemented with 10% FBS, 2mM L-glutamine, 1% 1M HEPES buffer and 1% penicillin-streptomycin. Cells were either cultured for 3 days at 37°C, 5% CO₂ in anti-CD3 (1ug/ml) coated petri dishes with 0.5 ug/ml of soluble anti-CD28 or in non-coated plates without anti-CD28.

Macrophage differentiation and polarization

Monocytes were isolated from PBMCs using plate adherence. PBMCs were plated in petri dishes and cultured for 3hrs in serum-free RPMI. Media was subsequently replaced with 10ml RPMI containing 10% FBS and 40ng/ml human macrophage colony stimulating factor. The cells were

cultured for an additional 5 days, at 37°C, 5% CO₂ and fed on day 1 by adding 10ml RPMI containing 40ng/ml M-CSF. For M2 polarization, cells were stimulated with human IL-4 at 20ng/ml for 16hrs prior to harvesting. On day 6, cells were harvested using trypsin (0.25%) and manual disaggregation.

Cell lines

Classical Hodgkin cell lines, L428, KMH2, HDLM-2, L540 and L1236 (DSMZ, German cell line collection), and the Burkitt cell line, Raji (DSMZ, German cell line collection), were cultured in RPMI-1640 supplemented with 10% FBS, 2mM L-glutamine, 1% 1M HEPES buffer and 1% penicillin-streptomycin. Jurkat-E6-hPD-1 is the Jurkat-E6 human T cell line transfected with human PD-1 cDNA in a pEF6 vector encoding Blastidicin resistance. Jurkat-E6-hPD-1 was cultured as above but supplemented with gentamycin (0.082mg/500ml of media). Prototype clone, 1964.7, was kindly provided by G. Freeman, DFCI.

CyTOF Data Acquisition

The samples were acquired on a Helios mass cytometer operating on software version 6.5.358 (Fluidigm). The instrument-automated full tuning protocol was performed daily within 8 hours of acquisition according to manufacturer specifications, and was validated with 4-element EQ-beads run at stock concentration. A flow rate of 30uL/min and event rate <1000 cells/second were used with manufacturer default settings for dual count detection. After acquisition, the data were normalized using bead-based normalization in 100 second intervals with a minimum of 50 beads per interval using the Helios software².

The data were gated to exclude residual normalization beads and debris. The absence of cisplatin uptake was used to identify viable cells and the detection of cleaved PARP to exclude apoptotic cells. Two populations were identified using Ir191/193, a DNA intercalator that binds to cellular nucleic acid - 'singlet' and 'non-singlets'. Events in the singlet population were selected for subsequent high dimensional analyses using X-shift with Vortex. The non-singlet cluster was analyzed separately using manual gating to first identify HRS cells on the basis of CD15 and CD30 expression. The HRS cell population was then exported and separated according to CD3⁺ expression (Figure 3A).

EBV-Encoded Small RNA *In Situ* Hybridization

For 6 of the primary cHL cases, EBV status was assessed by EBV-encoded small RNA (EBER) *in situ* hybridization. EBERs were performed on 4-µm thick tissue sections using the Leica Bond III automated immunostaining platform as per manufacturer's protocol. In brief, 600ng/mL fluorescein-conjugated oligonucleotide EBER probe was applied and detected with an anti-fluorescein antibody (Leica Biosystems). Slides were processed with the Leica Bond Polymer Refine detection kit (Leica Biosystems).

EBV PCR analysis

In the 1 case with no additional FFPE slides, we assessed EBV status by PCR. Viral DNA was extracted from the cell suspension used in the CyTOF analysis using Qiagen ultrasens viral kit according to the manufacturer's guidelines (Qiagen). The forward primer 5'-GGC CAG AGG TAA GTG GAC TTT AAT and the reverse primer 5'-GGG GAC CCT GAG ACG GG align to sequences in the EBV gene, EBNA1 (Integrated DNA technologies). The PCR reaction was

performed at 51°C for 35 cycles. The PCR products were resolved on a 1.5% agarose gel with the EBV-positive cell line Raji and 3 EBV-negative cHL cell lines serving as controls.

Immunohistochemistry

We also performed dual immunohistochemical staining of MHC class I (EMR8-5, 1:6000; Abcam, Cambridge, MA/USA) and PAX5 (BD Biosciences) using an automated staining system (Bond III; Leica Biosystems, Vista, CA/USA) according to the manufacturer's protocol. Stained slides were categorized as previously described using a three-tier scoring system of negative, decreased or positive^{3,4}. All cases were scored by an expert hematopathologist (S.J.R.).

References

1. Fluidigm. Maxpar panel designer; 2014.
2. Finck R, Simonds EF, Jager A, et al. Normalization of mass cytometry data with bead standards. *Cytometry A*. 2013;83(5):483-494.
3. Roemer MG, Advani RH, Redd RA, et al. Classical Hodgkin Lymphoma with Reduced beta2M/MHC Class I Expression Is Associated with Inferior Outcome Independent of 9p24.1 Status. *Cancer Immunol Res*. 2016;4(11):910-916.
4. Roemer MGM, Redd RA, Cader FZ, et al. Major Histocompatibility Complex Class II and Programmed Death Ligand 1 Expression Predict Outcome After Programmed Death 1 Blockade in Classic Hodgkin Lymphoma. *J Clin Oncol*. 2018;36(10):942-950.

A

Specimen	Morphologic Diagnosis	EBV Status
1	Classical Hodgkin lymphoma, mixed cellularity	Positive
2	Classical Hodgkin lymphoma, nodular sclerosis	Positive
3	Classical Hodgkin lymphoma, nodular sclerosis	Negative
4	Classical Hodgkin lymphoma, nodular sclerosis	Negative
5	Classical Hodgkin lymphoma, nodular sclerosis	Negative
6	Classical Hodgkin lymphoma, nodular sclerosis	Negative
7	Classical Hodgkin lymphoma, mixed cellularity	Negative

B

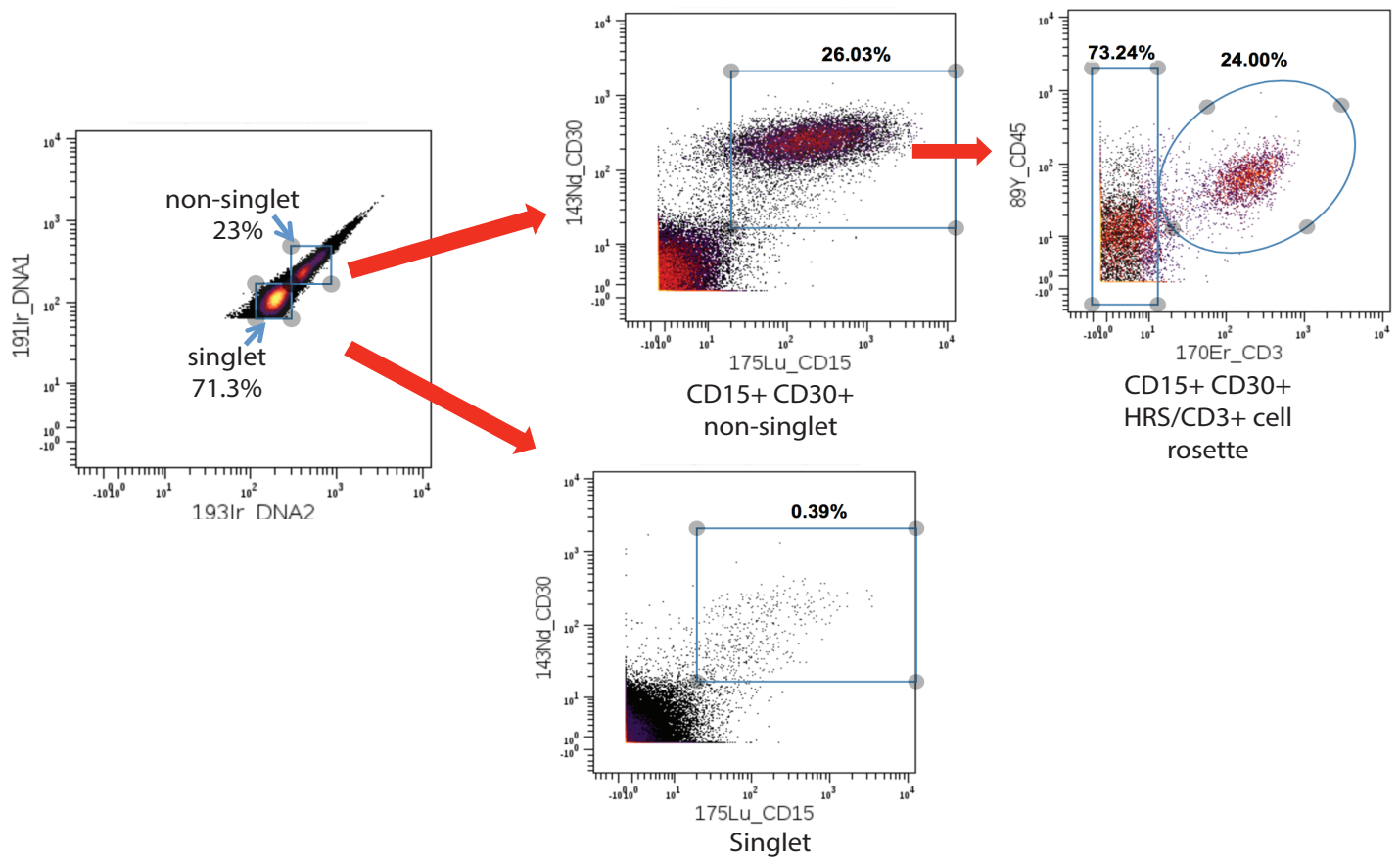
Specimen	Morphologic Diagnosis
300	Left tonsil
	Tonsil with chronic active inflammation-Lymphoid hyperplasia.
301	Lymph node
	Reactive lymph node with sinus histiocytosis and dermatopathic changes
302	Left inguinal lymph node
	Reactive lymph node with no morphologic or immunophenotypic evidence of lymphoma
304	Lymph node
	Lymph node with multiple foreign body-type, non-necrotizing granulomas. No neoplasm identified
305	Inguinal lymph node
	Reactive lymph node.
308	Cervical lymphadenopathy
	Reactive follicular hyperplasia.
309	Right axillary lymph node
	Reactive lymph nodes with follicular and interfollicular hyperplasia and no evidence of involvement of lymphoma.
310	Hilar lymph node
	Lymph node with reactive features.
311	Right tonsil
	Reactive follicular hyperplasia with focal active tonsillitis
312	Right tonsil
	Active tonsillitis with marked lymphoid hyperplasia and focal fibrosis

Supplemental Table 1. A) Histological diagnosis of primary Hodgkin lymphoma cases with EBV status
B) Histological diagnosis of reactive lymph nodes/tonsils.

Antibody	Source	Clone	Isotopes
CD45	Fluidigm/ DVS sciences	HI30	89Y
PAX5	Biologend	IH9	113Ind
CD14	Biologend	M5E2	115Ind
Eomes	eBioscience	WD1928	141Pr
Ki-67	BD Biosciences	B56	142Nd
CD30	BD biosciences	BerH8	143Nd
CCR5	Fluidigm/ DVS sciences	NP-6G4	144Nd
CD4	Fluidigm/ DVS sciences	RPA-T4	145Nd
CD8a	Fluidigm/ DVS sciences	RPA-T8	146Nd
cParp	BD Biosciences	F21-852	147Sm
HLA-A/B/C (MHC class I)	Biologend	W6/32	148Nd
CD25	Fluidigm/ DVS sciences	2A3	149Sm
CD57	Biologend	HCD57	150Nd
Tim3	BD biosciences	7D3	151Eu
PD-L2	Courtesy of G.Freeman, DFCI	24F.10C12	152Sm
pSTAT1	Fluidigm/ DVS sciences	4a	153Eu
CD163	Fluidigm/ DVS sciences	GHI/61	154Sm
PD-1	Courtesy of G.Freeman, DFCI	EH12.2H7	155Gd
B2M	Biologend	2M2	156Gd
CCR4	Fluidigm/ DVS sciences	205410	158Gd
CCR7	Fluidigm/ DVS sciences	G043H7	159Tb
T-bet	Fluidigm/ DVS sciences	4B10	160Gd
PD-L1	Courtesy of G.Freeman, DFCI	29E.2A3	161Dy
FoxP3	Fluidigm/ DVS sciences	PCH101	162Dy
CXCR5	BD biosciences	51505	163Dy
CD161	Fluidigm/ DVS sciences	HP-3G10	164Dy
CD45RO	Fluidigm/ DVS sciences	UCHL1	165Ho
Lag3	R&D	874501	166Er
Granzyme B	Harvard Medical School	GB11	167Er
CD73	Fluidigm/ DVS sciences	AD2	168Er
CD33	Fluidigm/ DVS sciences	WM53	169Tm
CD3	Fluidigm/ DVS sciences	UCH T 1	170Er
CD68	Fluidigm/ DVS sciences	Y1/82a	171Yb
phosphoS6	Cell Signaling Technologies	D57.2.2E	172Yb
IRF4	Biologend	IRF4.3E4	173Yb
HLA-DR/DP/DQ (MHC class II)	Biologend	Tu39	174Yb
CD15	Biologend	HI98	175Lu
CD56	BD Biosciences	B159	176Yb
CD16	Fluidigm/ DVS sciences	3G8	209Bi

Supplemental Table 2. Antibodies and clones used in the CyTOF panel

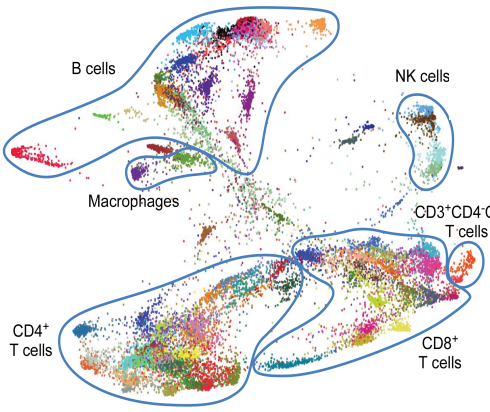
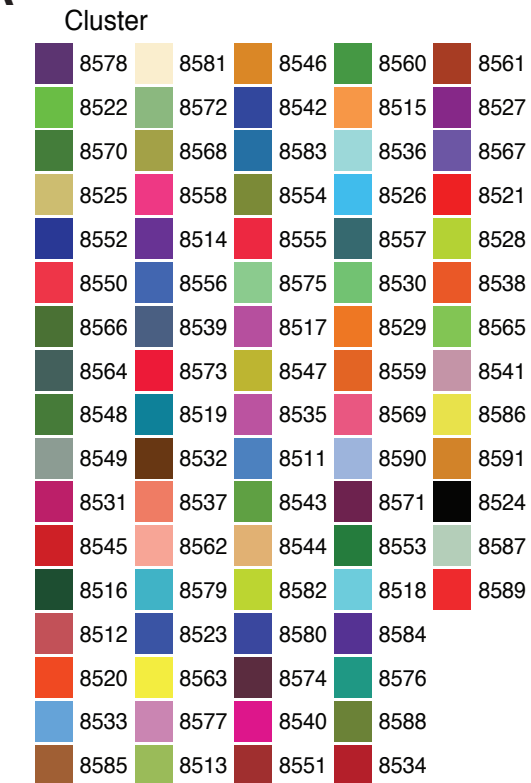
Supplemental Figure 1



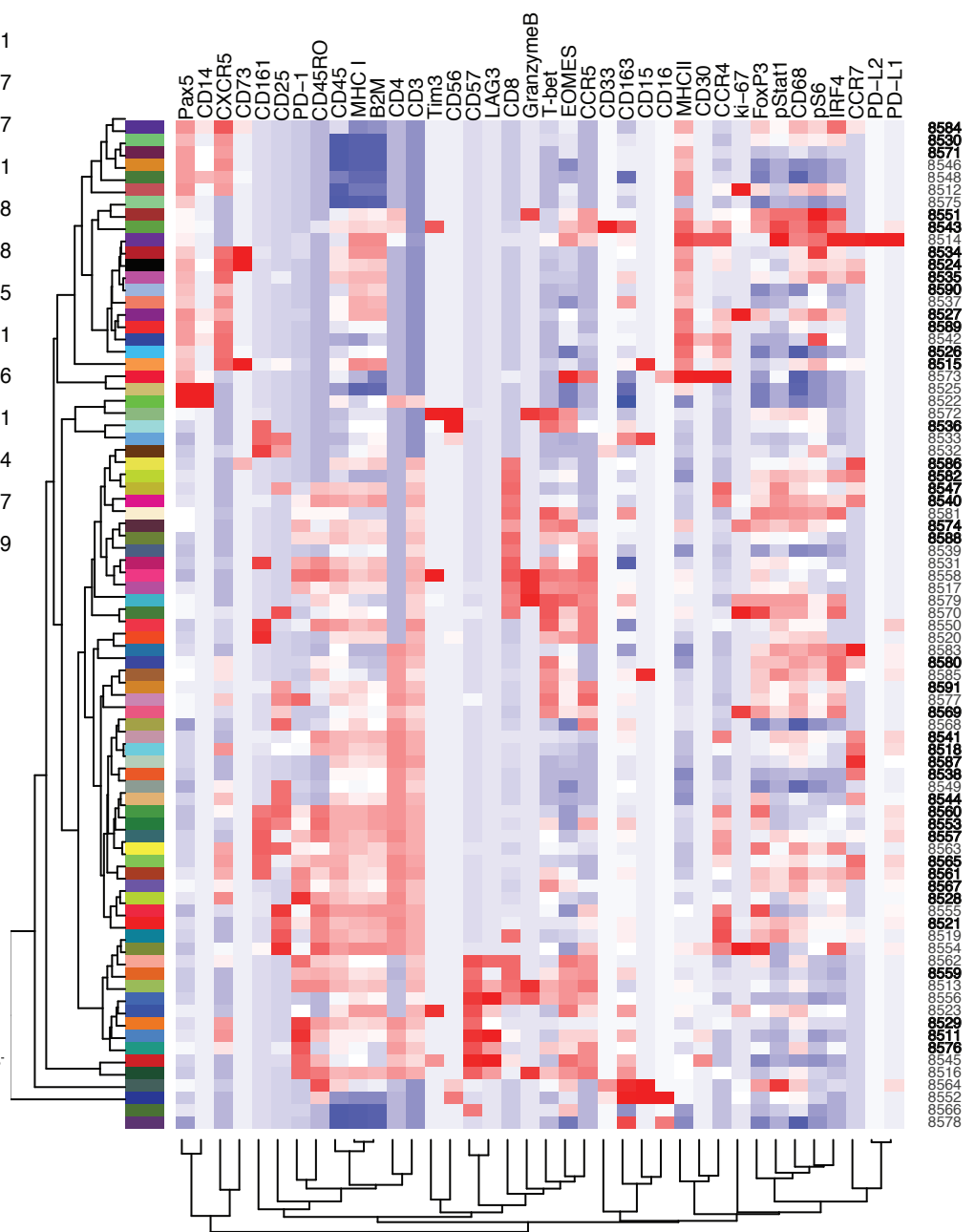
Supplemental Figure 1. HRS cells are detected in the non-singlet cluster and are rosetted by CD3+ T cells. An admixture of 75% peripheral blood mononuclear cells (PBMC) and 25% KMH2 cHL cells was stained using the described CyTOF protocol (Supplemental Methods). The DNA intercalator Ir 191/193 separates events into 2 groups, singlets and non-singlets. Gating for CD15+ and CD30+ indicates that the majority of KMH2 cHL cells reside in the non-singlet population. The CD15+CD30+ non-singlet population was further gated for CD3+ identifying a discrete population of Hodgkin Reed Sternberg (HRS) cell/CD3+ T-cell rosettes.

Supplemental Figure 2

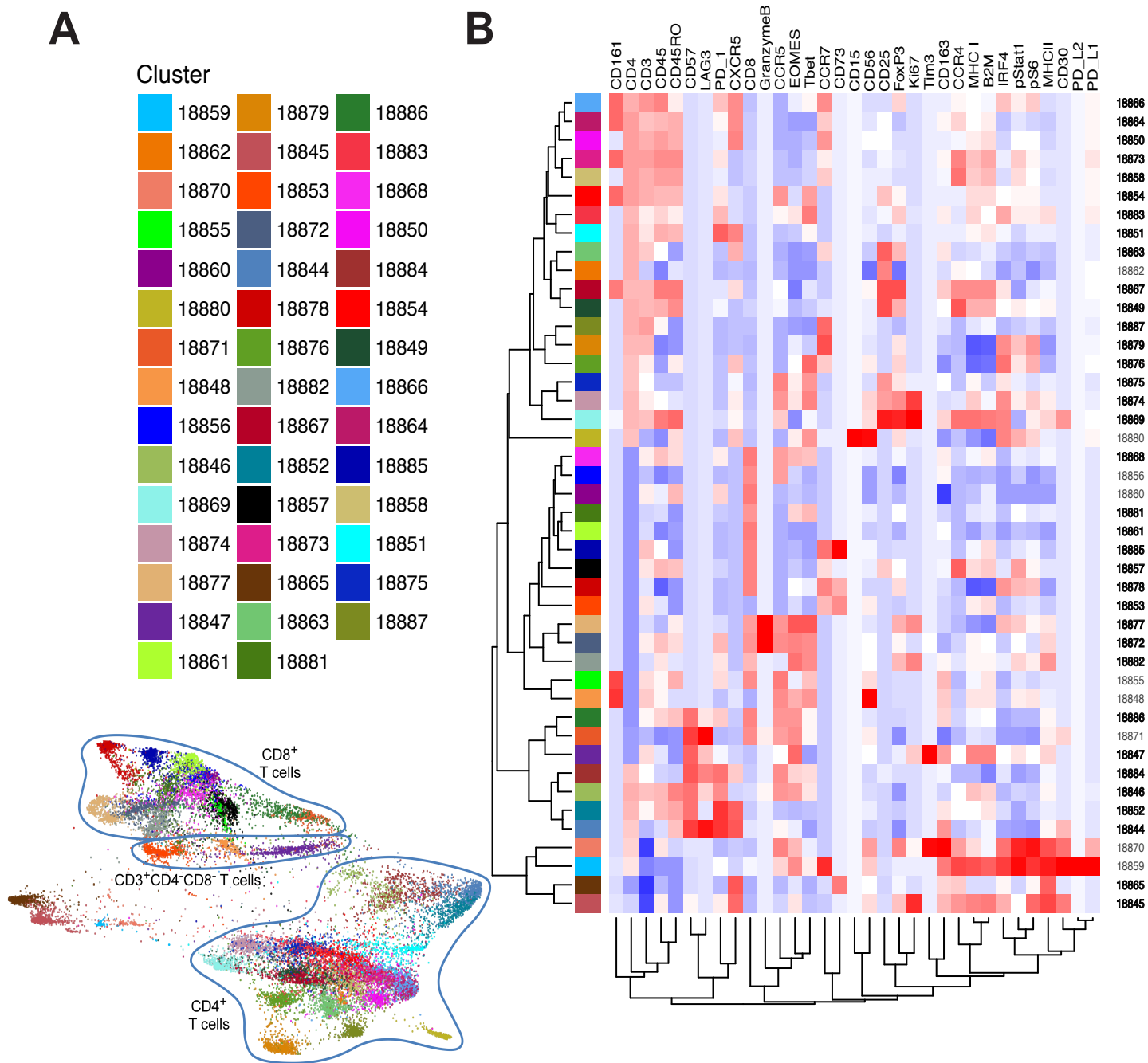
A



B

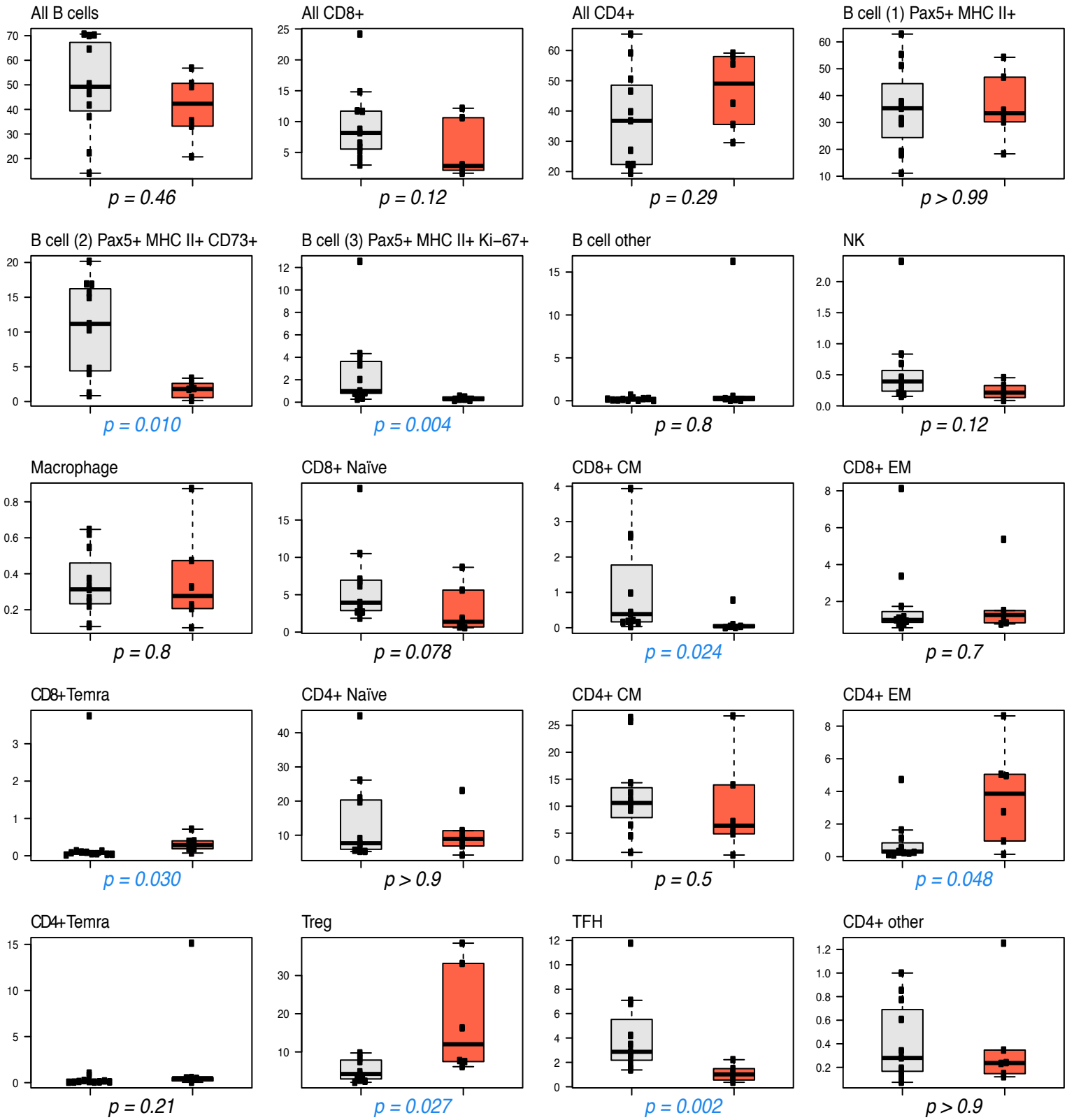


Supplemental Figure 2. CyTOF analyses of all viable cells. A) Every unique population identified from X-Shift analysis of viable singlet cells within the Vortex visualization environment is assigned a specific Hex color code. Shown are Hex color codes (upper) for every cluster in the FDL of all viable cells (lower). B) Heatmap of relative expression of each CyTOF panel protein, as defined by a z-score, for every cluster, including those with <5% sampled events/case. Cluster color codes on left, y-axis. Cluster IDs on right, y-axis; clusters with >5% of sampled events/case in bold. All cHLs and RLNTs are included.

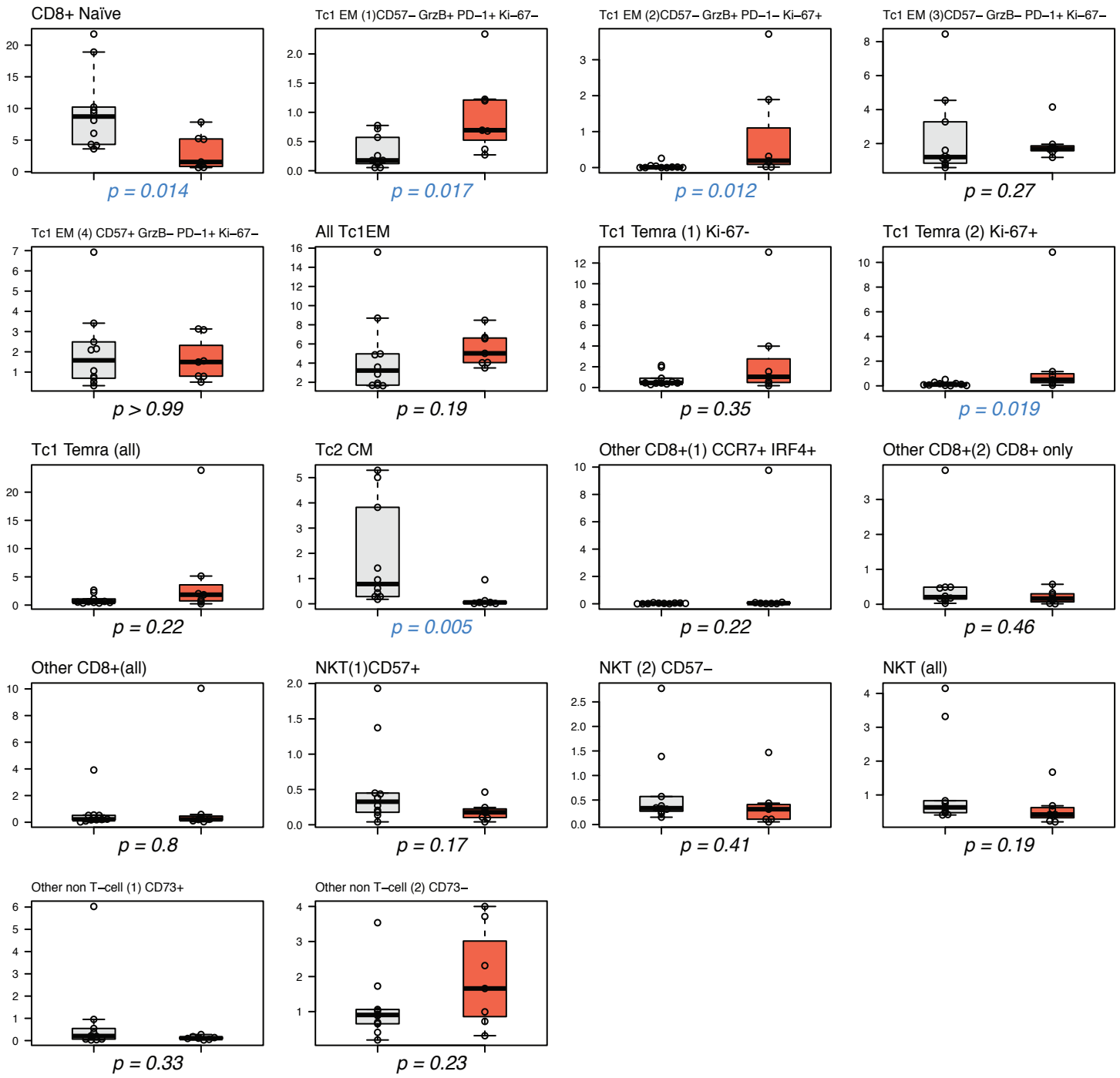


Supplemental Figure 3. CyTOF analyses of CD3+ cells. A) Every unique population identified from X-Shift analysis of CD3+ cells within the Vortex visualization environment is assigned a specific Hex color code. Shown are Hex color codes (upper) for every cluster in the FDL of CD3+ cells (lower). B) Heatmap of relative expression of each CyTOF panel protein, as defined by a z-score, for every cluster including those with <5% sampled events/case. Cluster color codes on left, y-axis. Cluster IDs on right, y-axis; clusters with >5% of sampled events/case including those with <5% sampled events/case. Cluster color codes on left, y-axis in bold. All cHLs and RLNTs are included.

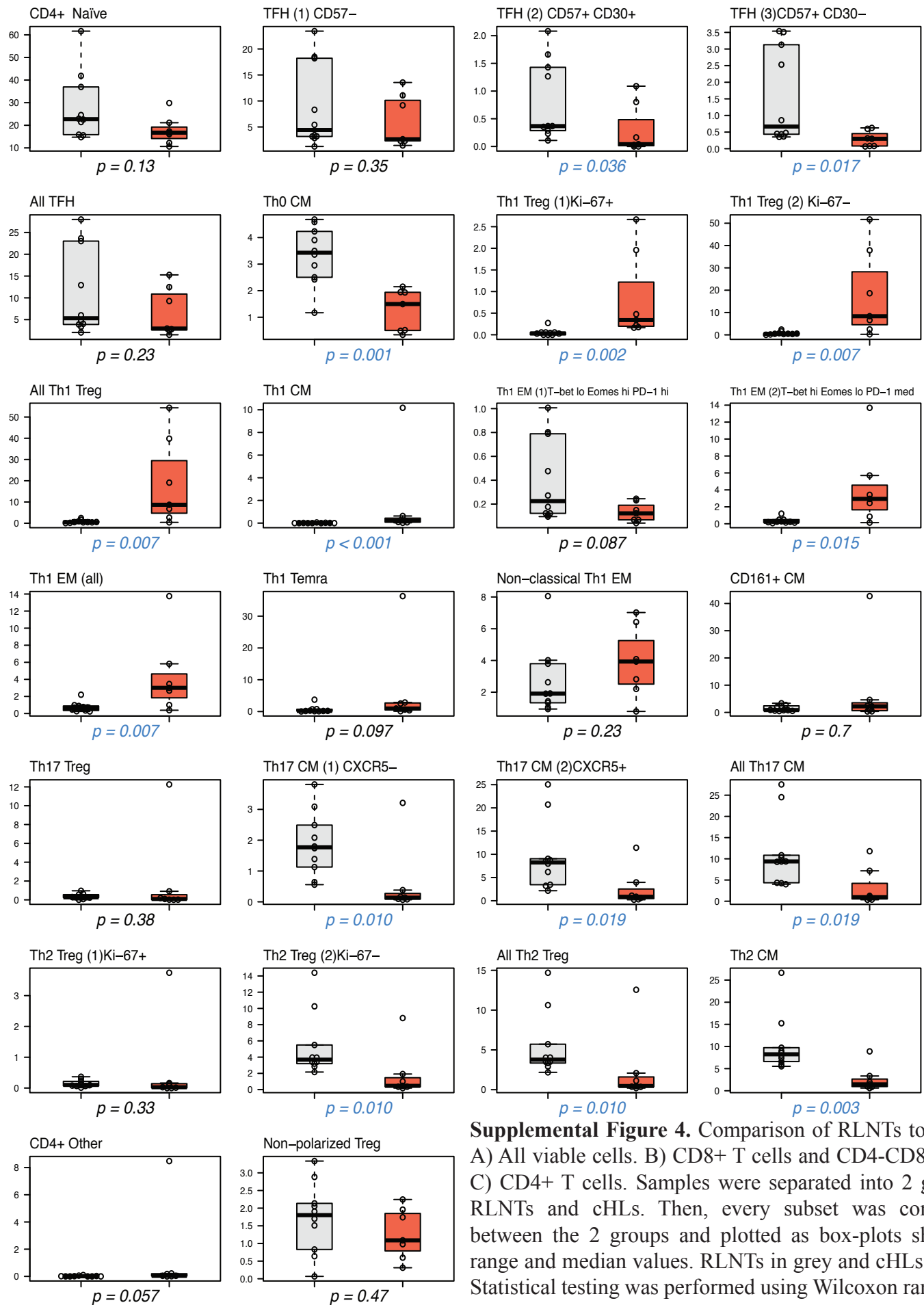
Supplemental Figure 4A



Supplemental Figure 4B

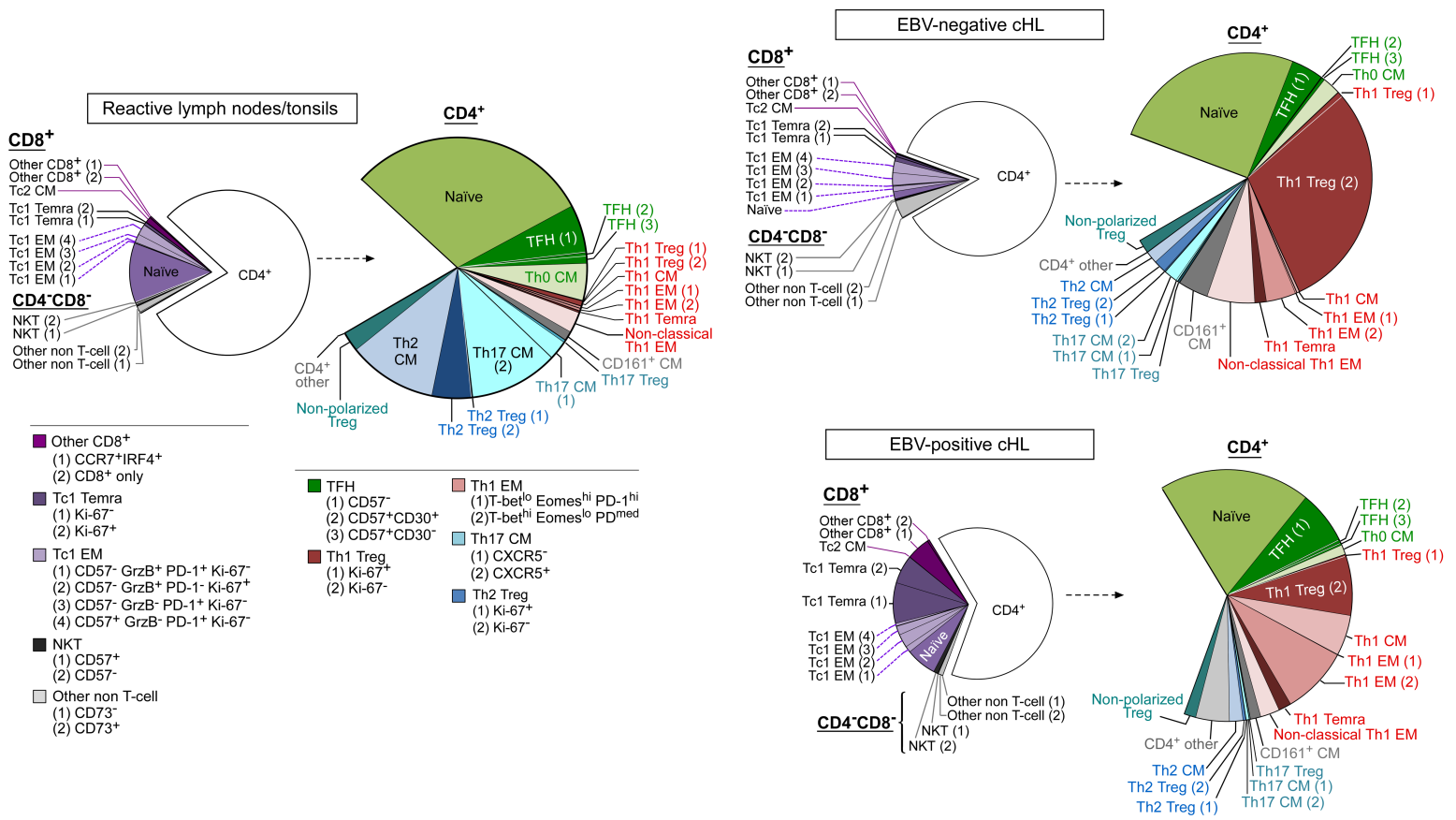


Supplemental Figure 4C



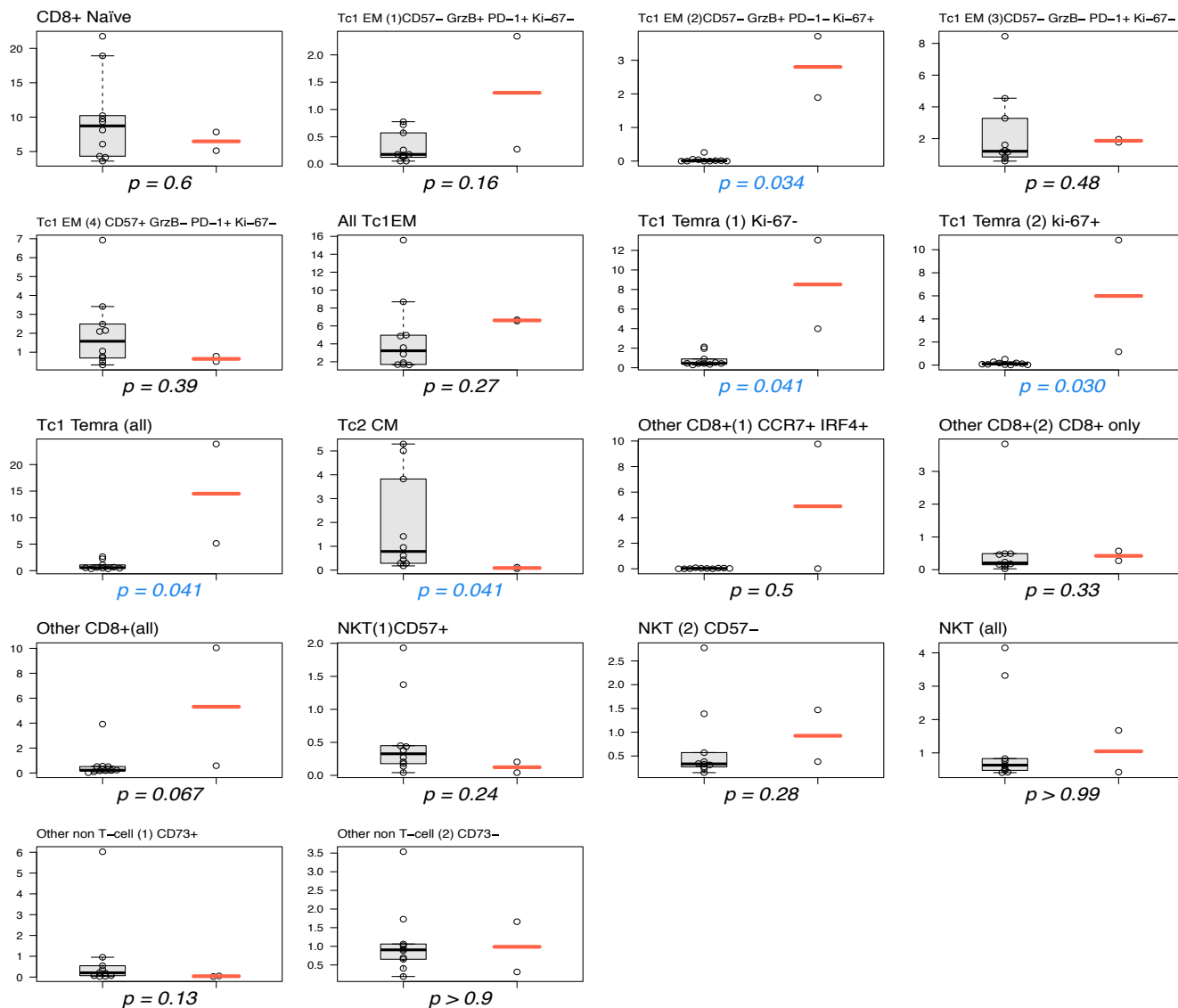
Supplemental Figure 4. Comparison of RLNTs to cHLs. A) All viable cells. B) CD8+ T cells and CD4-CD8- cells. C) CD4+ T cells. Samples were separated into 2 groups, RLNTs and cHLs. Then, every subset was compared between the 2 groups and plotted as box-plots showing range and median values. RLNTs in grey and cHLs in red. Statistical testing was performed using Wilcoxon rank-sum test. Nominal p values <0.05 indicated in blue

Supplemental Figure 5

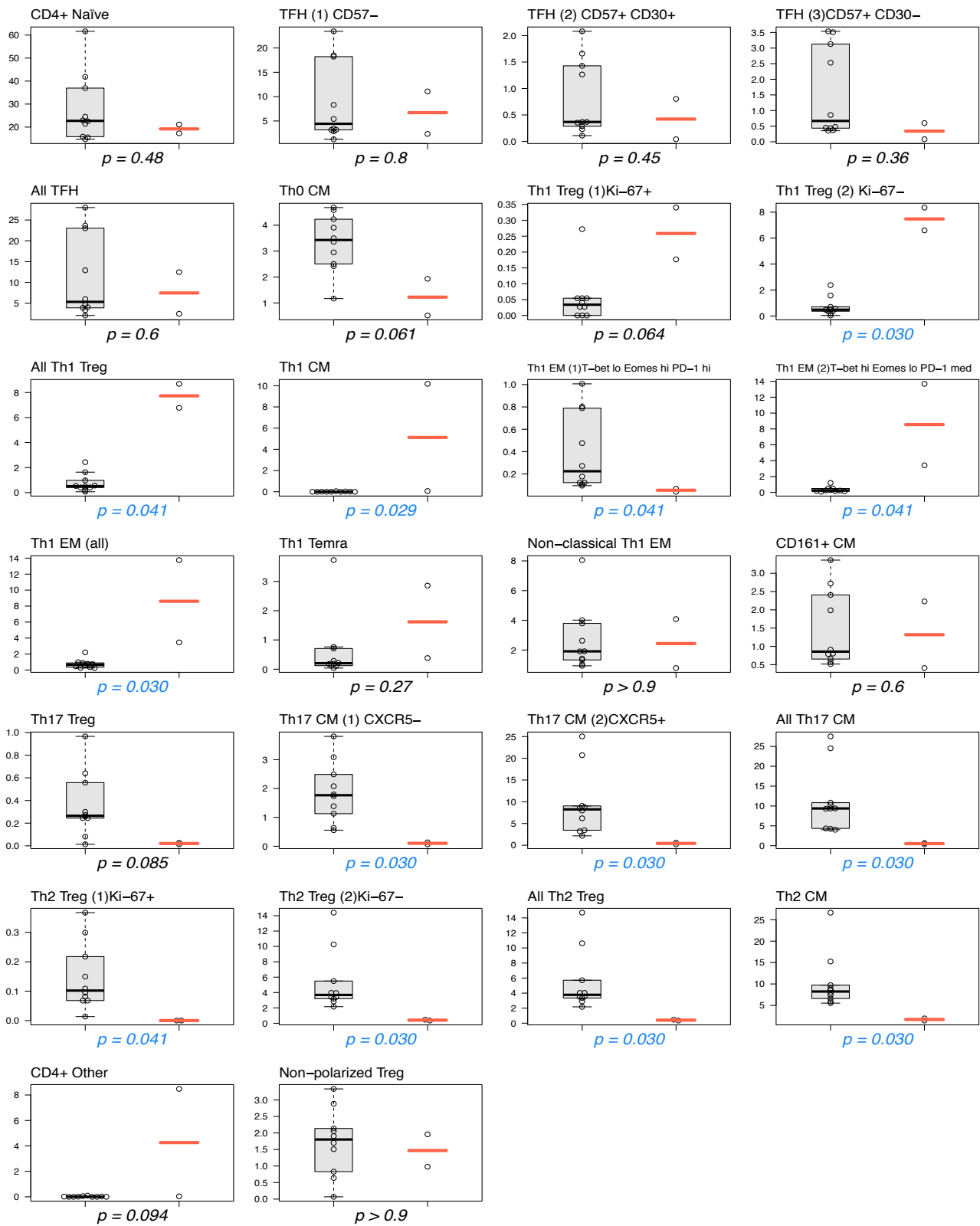


Supplemental Figure 5. Comparison of CD3⁺ cell composition in RLNTs and EBV-negative and EBV-positive cHLs. Every cluster with >5% of sampled events/case was phenotyped based on lineage, differentiation and polarization status. RLNTs (from Figure 7B) included on left for comparison. For each cluster and shared category in the RLNTs (left) and EBV-negative (right, top panel) and EBV-positive (right, bottom panel) cHLs, the median cell count was calculated and represented as comparison pie charts.

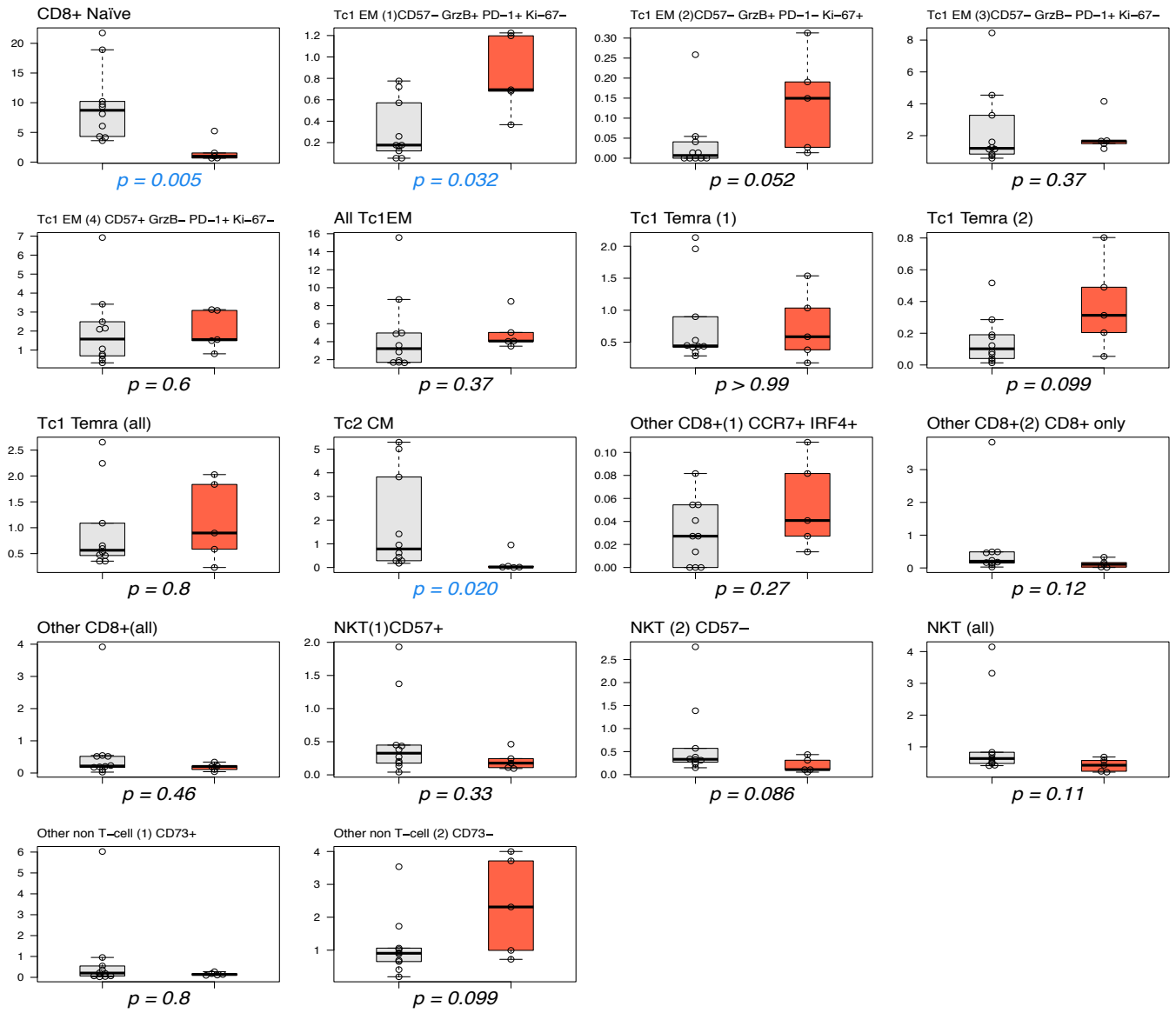
Supplemental Figure 6A



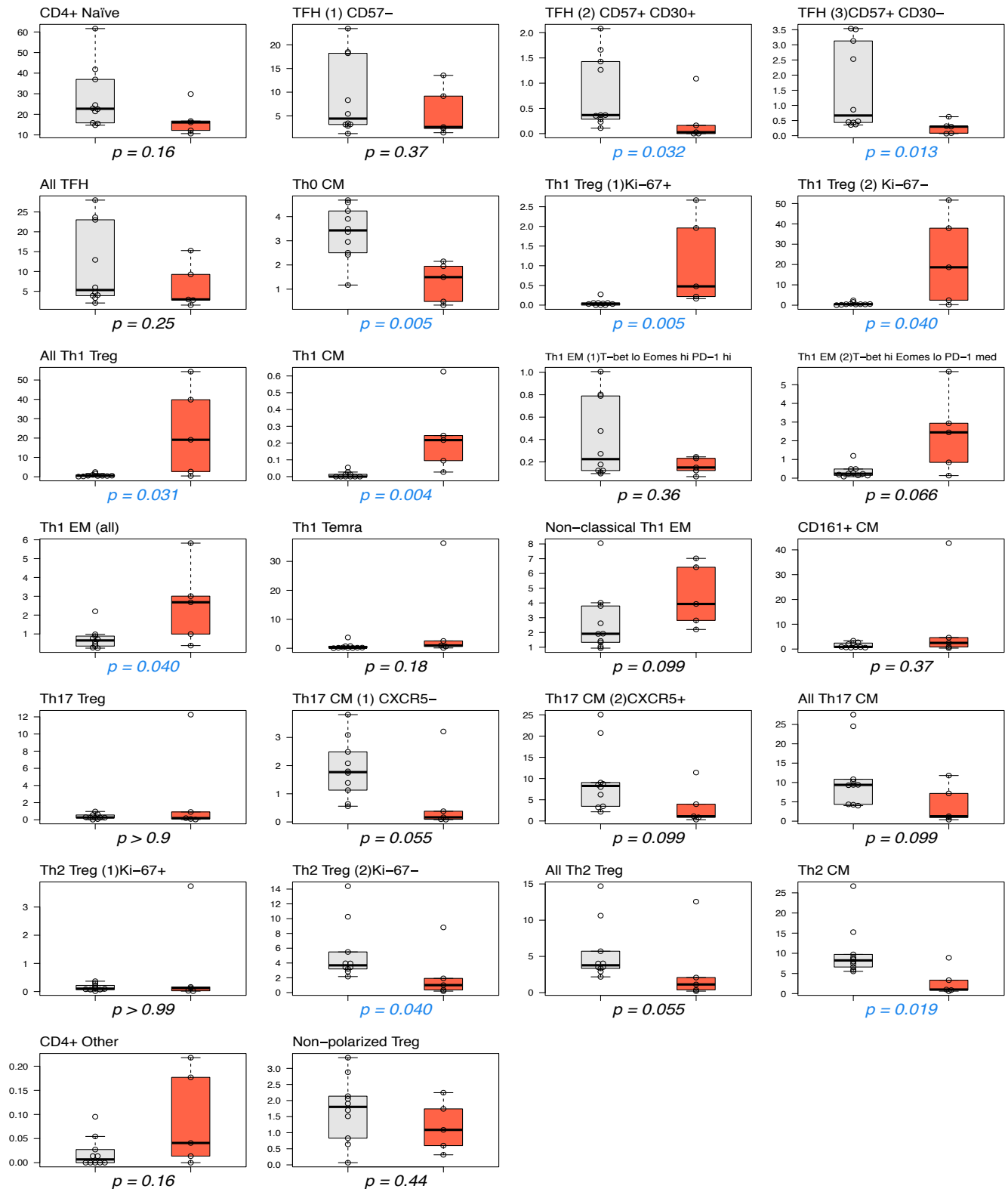
Supplemental Figure 6A (continued)



Supplemental Figure 6B



Supplemental Figure 6B (continued)



Supplemental Figure 6. Comparison of CD3+ subsets. A) RLNTs versus EBV-positive cHLs B) RLNTs versus EBV-negative cHLs. Box-plots showing range and median values of every CD3+ subset. Statistical testing performed using Wilcoxon rank sum test. Nominal p values < 0.05 in blue.